JOURNAL OF CATALYSIS **170,** 150–160 (1997)
ARTICLE NO. CA971745

Isoprene by Prins Condensation over Acidic Molecular Sieves

E. Dumitriu,* D. Trong On,† and S. Kaliaguine†,[1]

Laboratory of Catalysis, Technical University of Iasi, 71 Prof. D. Mangeron, Iasi-6600 Romania; and †Department of Chemical Engineering, Laval University, Quebec, G1K 7P4 Canada

Received December 2, 1996; revised April 7, 1997; accepted May 5, 1997

The Prins condensation of isobutylene with formaldehyde over different catalysts (HY, USY, H-ZSM-5, H-Boralite, H-B-MCM-41) having various pore sizes and acidities has been investigated in a pulse microreactor. The results show unambiguously that high selectivities to isoprene are obtained only in the presence of weakly acidic Brønsted acid sites. © 1997 Academic Press

INTRODUCTION

The Prins condensation of olefins with aldehydes is considered to be an important organic reaction, since it allows one to obtain various unsaturated alcohols, glycols, acetals, and other valuable compounds. This condensation is typically catalyzed by strong mineral acids such as H_2SO_4 in homogeneous catalysis (1), but in some applications, e.g., the synthesis of isoprene, an increasing interest in heterogeneous catalysis must be noted (2–7).

For isoprene synthesis the most promising results have been obtained using zeolites as catalysts. The reaction network shown in Fig. 1 was suggested for the reaction of isobutylene and formaldehyde using 12- and 10-ring zeolites (8).

If, over 12-ring zeolites route (a) is favored, when the condensation is performed over 10-ring zeolites, in accord with expected shape-selective constraints, less 4,4-dimethyl-1,3-dioxane is formed, and route (b) can be considered as favored. The condensation reaction usually proceeds by route (c) at low temperatures. Moreover, as previously shown (6, 7), this network is complicated by a parallel network involving the oligomerization-cracking reactions of the olefins and dienes, as well as their aromatization.

Therefore, producing isoprene selectively is a difficult task, since the ideal catalyst must assure a high selectivity not only for the primary Prins condensation to isoprene, but for the entire process. The aim of the present study is to compare the relative importance of acidic properties and pore geometry to catalyst selectivity in this reaction. These parameters are varied by changing the catalyst from Y zeolites to H-ZSM-5, boralites, and boron-MCM-41.

EXPERIMENTAL

Y zeolites. Ultrastable Y zeolites with different Si/Al ratios were provided by PQ Zeolites B.V. (Table 1). HY zeolites were prepared by calcination of an ammonium-exchanged sample. These samples (except USY-28) were described in a previous publication (18).

H-ZSM-5 zeolites. Two samples with respective Si/Al of 17.5 and 37.5 were purchased from PQ Zeolites in their ammonium form. Samples with higher Si/Al ratios ranging from 110 to 500 were synthesized by a hydrothermal procedure, using an aerosil as the silicon source, aluminum hydroxide, $Al(OH)_3$ (Merck) as the aluminum source, sodium hydroxide and TPABr as the template. These samples were calcined at 873 K and ion exchanged three times at 363 K in a 0.1 *M* solution of ammonium chloride, filtered and washed, and then dried and recalcined at 873 K for 6 h (7).

Boralites. A series of boralites with different boron contents were prepared from tetraethylorthosilicate (TEOS), boric acid (H_3BO_3), tetrapropylammonium hydroxide (TPAOH), and water by a method described previously (9, 10). The composition of the alkali-free gel was SiO_2–xB_2O_3–0.40 TPAOH-35 H_2O (where $x = 0.1-0.5$). The gel was charged in a Teflon-lined autoclave and maintained under hydrothermal conditions for 5 days at 448 K. The solids were filtered, washed with distilled water, dried at 357 K, and calcined in a horizontal tubular quartz reactor under a continuous flow of either dry ammonia or air at 823 K for 6 h (heated from room temperature to 823 K at the heating rate of 2 K/min).

Ammonium and sodium exchange were carried out by stirring 0.5 g of boralite (which was treated in NH_3 at 450°C for 4 h) in 30 ml of 1 mol liter^{-1} aqueous ammonium nitrate and sodium bromide solutions, respectively, for 24 h at room temperature.

B-MCM-41. The hydrothermal synthesis of B-MCM-41 was carried out using gels with the molar composition SiO_2–$0.05B_2O_3$–0.27CTACl–$0.13Na_2O$–0.26TMAOH–$0.27NH_4OH$–$60H_2O$ (CTACl, cetyltrimethyl ammonium chloride; TMAOH, tetramethylammonium hydroxide). A typical synthesis procedure was described earlier (11, 12).

---

[1] To whom correspondence should be addressed.

0021-9517/97 $25.00

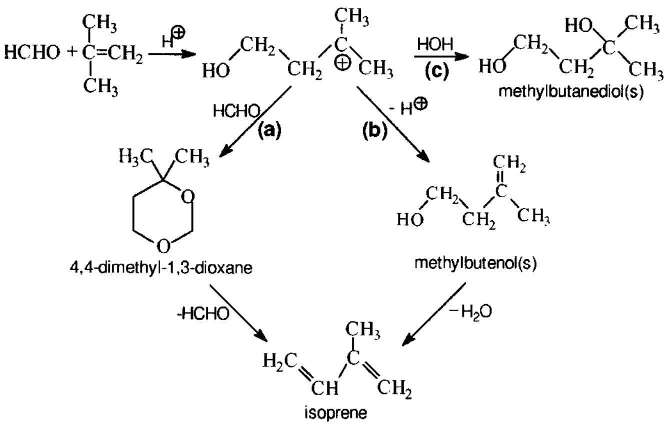

FIG. 1. Reaction pathways for Prins condensation of formaldehyde and isobutene over various acidic 12- and 10-ring zeolites.

The homogeneous gel was transferred into a Teflon-lined autoclave and heated to 423 K for 48 h. The solid products were filtered, washed with distilled water, dried in air at 353 K, and finally calcined in flowing air at 813 K for 6 h (heated from room temperature to 813 K at the heating rate of 1 K/min). The pure-silica MCM-41 was synthesized using the same procedure, except that no boron was added.

Elemental analysis was performed by atomic absorption spectroscopy for sodium and silicon, whereas ICPAES (induced coupled plasma atomic emission spectroscopy) was used for boron estimation. Powder X-ray diffraction patterns of the samples were recorded on a Rigaku D-MAX II VC X-ray diffractometer using nickel-filtered Cu$K\alpha$ ($\lambda = 1.5406$ Å) radiation. Surface area measurements were carried out using an Omnisorp-100 apparatus following the BET procedure. IR spectra were recorded on a Digilab FTS-60 spectrometer, using wafers of 10 mg cm^{-2} treated in a vacuum cell at 773 K for 4 h. The samples were cooled to room temperature under vacuum and then immediately exposed to pyridine vapour for 15 min. Desorption of pyridine was carried out by evacuation for 4 h at different temperatures. ^{11}B MAS–NMR measurements were performed at room temperature on a Bruker ASX 300 spectrometer at a resonance frequency of 96.25 MHz. ^{11}B MAS–NMR spectra were obtained with a 90°-pulse duration of 2.5 μs, repetition time of 2 s, and spinning rate of 3.5 kHz. Chemical shifts were determined relative to $BF_3 \cdot O(C_2H_5)_2$.

TABLE 1

The Main Characteristics of Y Faujasites

Sample	SiO_2/Al_2O_3 molar ratio	Unit cell size (Å)	Surface area (m^2 g^{-1})
HY	4.6		
USY-5	5.2	24.33	660
USY-11	11.5	24.33	730
USY-28[a]	28.2		
USY-80	80	24.25	780

[a] By steaming of USY-11.

Reagents. *Tert*-butyl alcohol (TBA), Fluka p.a., was used to generate *in situ* isobutylene (iB). Fresh aqueous solutions of formaldehyde were prepared by the thermal depolymerization of paraformaldehyde. The concentration of formaldehyde (34 wt%) was determined by chemical methods.

Catalytic tests. The condensation reaction was carried out in a pulse microreactor under the following conditions: weight of catalyst 0.04 g (granules of pure sieves, 0.25–0.5 mm grain size); nitrogen flow rate 20 ml/min, unless otherwise indicated; pulse size 0.4 μl; equimolar reaction mixture, unless otherwise stated. The liquid reagents were fed to the reactor via an injector maintained at the reaction temperature. Separate tests were performed, which showed that for all tested catalysts a pulse of pure TBA is totally dehydrated to isobutylene at temperatures above 443 K. The reaction products were analyzed using an on-line GC with FID or TCD and various columns. A detailed description of the catalytic tests is given in an earlier paper (6).

CHARACTERIZATION RESULTS

As mentioned above, descriptions of the Y and the ZSM-5 samples were reported previously (7, 18). Results obtained with these samples are reported here for comparison with H-boralites and H-MCM-41. Thus only a detailed characterization of the latter two types of catalysts is reported here.

Boralites

X-ray diffraction. The X-ray diffraction (XRD) pattern of the boralite sample is characteristic of the orthorhombic MFI structure. Considering the boron-free silicalite as 100% crystalline, the crystallinity of boronsilicalite samples was found to be 95 ± 5%. The unit cell parameters were calculated from Rietveld refinement of the powder patterns using silicon as an internal reference. The 2.9% boron leads to a decrease of the unit cell from 5335 Å^3 for the boron free silicalite to 5280 Å^3 (Table 2), which is consistent with previous reports (13). This observation is logical on account of B–O bond being shorter (1.47 Å) than Si–O (1.61 Å) and thereby supports the incorporation of boron in the framework lattice.

Framework IR. Typical IR spectra of the as-synthesized and calcined boralite samples are given in Fig. 2. In all cases, the IR spectra were typical of pentasil zeolites. The well-defined IR bands at 800 and 455 cm^{-1} and the saturated one in the 1000–1300 cm^{-1} range are characteristic of SiO_4

TABLE 2

Concentrations of the Boron Species in Boralites (BS), as Determined by ^{11}B MAS–NMR and Chemical Analysis

	NMR				
Sample[a]	Line 1[b] (∼−3.7 ppm)	Line 2 (∼−2.0 ppm)	Line 3 (∼6 ppm)	Total	Chemical analysis
	B/u.c	B/u.c.	B/u.c.	B/Si (%)	B/Si (%)
[as-synth]BS-8.5	3.8	0.3	0.6	4.9	8.5
[as-synth]BS-4.0	3.5	0.4	—	4.2	4.0
[NH_4^+]BS-3.9					3.9
[H^+]BS-3.8					3.8
[Na^+]BS-3.4					3.4
[as-synth]BS-3.0	2.8	0.1	—	3.2	3.0
[H^+]BS-2.9	2.1	—	0.1	2.3	2.9
[H^+]BS-2.4[c]	1.7	—	—	1.8	2.4
[as-synth]BS-2.0					2.1
[H^+]BS-2.0					2.0
[as-synth]BS-1.5	1.4	0.1	—	1.6	1.5
[Na^+H^+]BS-1.5	1.0	0.4	—	1.5	1.5
[H^+]BS-1.5					1.5

[a] Sample referred to as [f] BS-r, where f and r are the form and B/Si ratio (%) of boralite, respectively.

[b] Amounts estimated by using the calibration curve for framework tetrahedral boron at −3.7 ppm. The values of the line at ∼−2 ppm might not be quantitative and are given as trend.

[c] Washed with distilled water.

tetrahedron units, while the vibrational mode at 555 cm^{-1} attests the presence of the five member rings of the pentasil silicalites. In addition to the intense absorption of pentasils, the as-synthesized sample exhibits weak bands (1470, 1455, and 1380 cm^{-1}) due to TPA$^+$. Upon ammonia treatment (Fig. 2b), residual TPA$^+$ (1380, 700, and 670 cm^{-1}) is also seen (14). The band at 920 cm^{-1} can be assigned to the presence of the tetracoordinated framework boron and it is observed in all boron pentasils. However, for the calcined sample a strong band also appears at 1380 cm^{-1}, which can be assigned to tricoordinated framework boron (9, 10, 15). The transformation of the absorption band at 920 cm^{-1} to one at 1380 cm^{-1} upon calcination is logically assigned to the change of boron coordination from tetrahedral to trigonal. On the other hand, after the NH_3 treatments (Fig. 2b), followed by Na^+-exchange (Fig. 2c) and calcination (Fig. 2d), the IR spectra do not show the characteristic BO_3 absorption at 1380 cm^{-1} consistently with the literature (15). It is concluded that tetrahedral framework boron is stable when NH_4^+ or Na^+ ions are counterbalancing the framework negative charge and unstable when the counterion is the proton (Fig. 2e) (9, 15, 19).

NMR. Figure 3 shows the ^{11}B NMR spectra of as-synthesized and calcined BS-3.0 samples. A single narrow peak observed at ∼4.0 ppm for the as-synthesized sample confirms that most of the boron has been incorporated as tetrahedral BO_4 units in the framework. Two very broad lines of much weaker intensity around −2 ppm correspond to framework-linked trigonal boron (9, 10, 15). Upon removal of the template after calcination in flowing oxygen the intensity of the line representing the tetrahedral framework boron is decreased and is slightly shifted to −3.7 ppm, while the trigonal framework boron lines are relatively increased, with an extra hump appearing at 6 ppm (Fig. 3b). This transformation is due to the loss of framework boron during calcination (Fig. 3 and Table 2). The additional hump at ∼6 ppm can be assigned to extraframework trigonal boron, consistently with the same signal obtained for silicalite impregnated with boric acid $B(OH)_3$. The observed

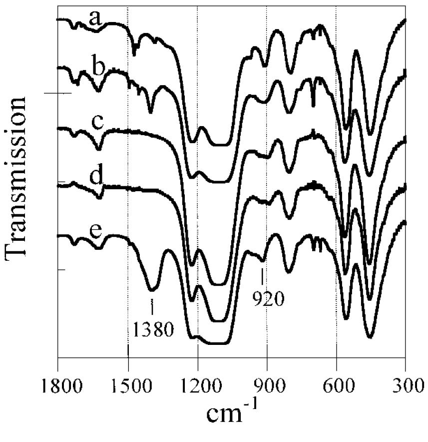

FIG. 2. IR spectra of the boralites: (a) as-synthesized BS-40, (b) [NH_4^+]BS-3.9, (c) [Na^+]BS-3.4 before calcination, (d) [Na^+]BS-3.4 after calcination at 823 K, and (e) [H^+]BS-3.8 before calcination.

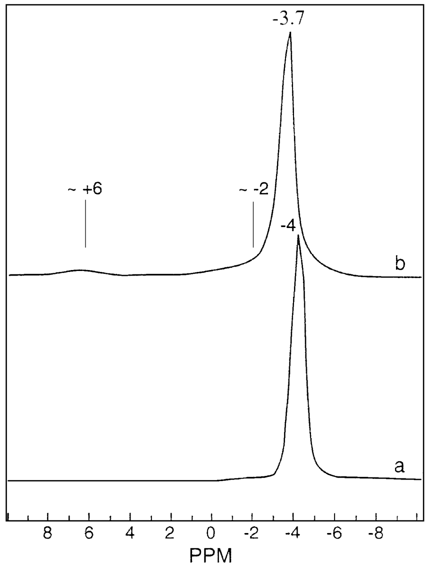

FIG. 3. ^{11}B MAS–NMR spectra of boralite, BS-3.0: (a) as-synthesized and (b) calcined sample.

small shift at lower fields (from −4.0 to −3.7 ppm) for the tetrahedral boron signal after different treatments can be explained by a change in the chemical environment (10, 15).

As the NMR line at ∼−3.7 ppm is very sensitive to the local structure and the electronic environment, a quantitative determination of tetrahedral boron content in the studied samples can be made by measuring the intensity of the NMR line at −3.7 ppm and using a calibration curve such as the one in Ref. (10). Table 2 reports semiquantitative information on other estimated boron states. The total boron content does not change much during the different treatments as observed by chemical analysis. The extraframework and trigonal boron are, however, strongly affected by various postsynthesis treatments as seen from ^{11}B NMR. They can for example be extracted from the MFI channels by washing at room temperature with distilled water (Table 2, sample BS-2.4).

The ^{11}B NMR spectra are similar for the as-synthesized and NH_3 calcined samples. The amount of trigonal boron only slightly increases during the NH_3 treatment; NH_4^+ cation is charge balancing and, consequently, BO_4 is stable (Table 2). After Na-exchange with aqueous 1 *M* NaBr at room temperature, the trigonally coordinated framework boron signal disappears. A small amount of boron is, however, extracted again after the ammonia treatment. No loss of framework boron can be observed in the sodium form before and after calcination.

MCM-41 Materials

The chemical composition of solids and the BET surface area of B-MCM-41 and its pure silica analogue are summarized in Table 3. BET surfaces were 950 and 900 m^2/g for the pure silica and B-MCM-41, respectively. The X-ray diffraction pattern of the calcined B-MCM-41 sample matches well that of the calcined boron free silica MCM-41 and also the patterns reported by Kresge *et al.* (16). One major peak at 2θ ∼1.6 and three peaks at 2θ ∼2.8, 3.3, and 4.61 were observed. Beck *et al.* (20) indexed these peaks for a hexagonal arrangement of unidimensional pores.

^{11}B MAS–NMR spectra of the as-synthesized and calcined forms of B-MCM-41 are shown in Fig. 4. Only one peak at −2.5 ppm was exhibited by the as-synthesized sample, indicating only the presence of tetrahedral boron species. The ^{11}B MAS–NMR spectrum of the calcined sample shows the simultaneous presence of both tetrahedral and trigonal framework boron.

TABLE 3

Chemical Composition (Atomic Ratio) and Structural Properties of the Calcined MCM-41 Materials

Catalyst	M/Si^a (%)	Na/M (%)	XRD d_{100} d-spacing (Å)	BET surface area (m^2/g)
Pure silica MCM-41	—	—	57	950
B-MCM-41	2.4	30	55	900
Al-MCM-41	4.5	50	∼60	650

[a] M = B and Al, as per catalyst designation.

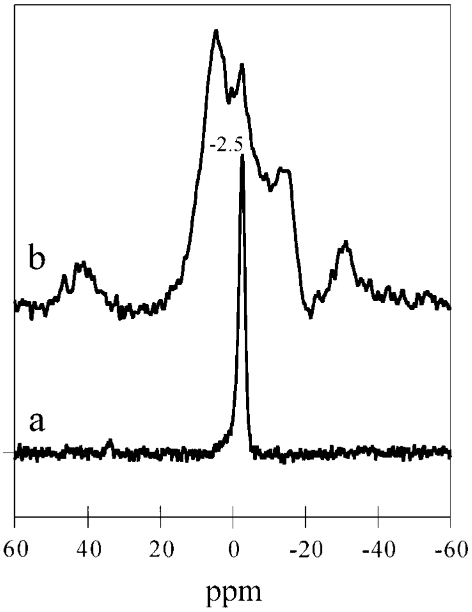

FIG. 4. ^{11}B MAS–NMR spectra of B-MCM-41: (a) as-synthesized and (b) calcined sample.

Acidity

Figure 5 shows the IR spectra of pyridine adsorbed on pure silica MCM41, B-MCM-41, Al-MCM-41 and Fig. 6

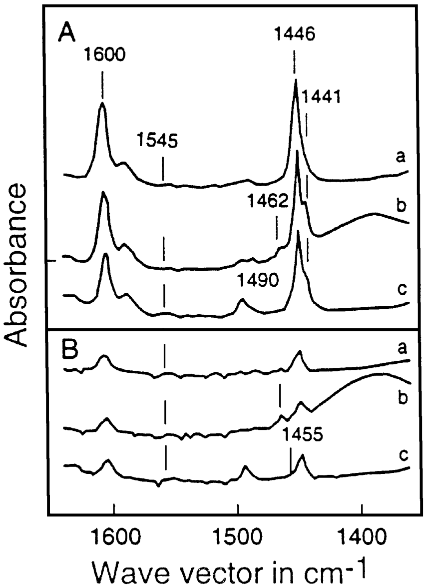

FIG. 5. IR spectra of pyridine after desorption at (A) 323 K and (B) 373 K: (a) pure silica MCM-41, (b) B-MCM-41, and (c) Al-MCM-41.

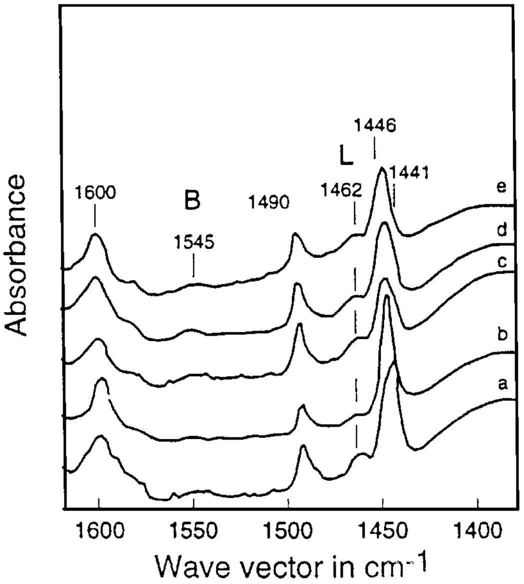

FIG. 6. IR spectra of pyridine on boralite, BS-3.0 after desorption at different temperatures: (a) room temperature, (b) 323 K, (c) 423 K, (d) 473 K, and (e) 573 K.

shows the IR spectra of boralites all pretreated under similar conditions in the IR cell. The [H^+]BS-2.9 sample of boralite containing 2.9 at% B was studied for comparison with the MCM-41 analogues. The IR broad band at 1380 cm^{-1} characteristic of framework trigonal boron as well as the 920 cm^{-1} peak characteristic of framework boron was observed for this sample. It is seen that pyridine adsorbed on the pure silica MCM-41 sample exhibits IR bands at 1441, 1446, and 1600 cm^{-1}. The bands at 1441 and 1600 cm^{-1}, which are characteristic of physisorbed pyridine, decreased sharply upon evacuation at 373 K. The band at 1446 cm^{-1} has been assigned to hydrogen-bonded pyridine (hydroxyl groups which do not protonate pyridine). The B-MCM-41, Al-MCM-41 and B-MFI samples show additional bands which are absent in pure silica MCM-41 (Figs. 5 and 6). Two very weak bands at 1545 and 1455 cm^{-1}, which are characteristic of Brønsted-acid and Lewis sites were observed in the IR spectrum of Al-MCM-41, as well as another band due to contributions of both Brønsted-acid and Lewis sites at 1492 cm^{-1}. The B-MCM-41 sample exhibited a very weak band at 1545 cm^{-1} and a new band at 1462 cm^{-1}; the latter has been assigned to strong Lewis sites generated by the polarization effect of hydroxyl nests and/or an electrophilic B atom (Figs. 5 and 6) (17).

The IR spectra of the B-MFI sample showed the bands at 1446, 1462, 1490, 1545, and 1600 cm^{-1}, even after evacuation at 573 K, while these bands had disappeared in B-MCM-41 and Al-MCM-41 samples, upon evacuation at lower temperature, ca. 373 K (Figs. 5 and 6). Finally, weak and mild acid sites (Brønsted and Lewis) were detected in the B-MCM-41 and the Al-MCM-41 samples. However, the B-MCM-41 IR spectrum exhibits a new band at 1462 cm^{-1}, indicating a higher amount of Lewis sites as compared to the Al-MCM-41. The acid strength of B-MCM-41 sample was found almost identical with that of the Al-MCM-41 sample. The B-MFI sample has a stronger acidity and a higher amount of acid sites than B-MCM-41 and Al-MCM-41. From the thermal stability of chemisorbed pyridine, the order of acid strength is found to be pure silica MCM-41 $<$ B-MCM-41 $\leq$ Al-MCM-41 $\ll$ B-ZSM-5.

REACTION RESULTS

As shown previously (6, 7), the condensation of formaldehyde with isobutylene can proceed over solid acid catalysts like zeolites, but it is well known that the acidity of a zeolite is connected with its behavior as catalyst in a complex fashion. Therefore, it is essential to analyze this behavior in relation to the nature, the number, and the strength of acid sites present in zeolites and molecular sieves.

Prins Condensation over Faujasites

The ability of zeolites to catalyze the Prins condensation was established for the first time by Venuto and Landis (2), when this reaction was performed on Y faujasite. Unfortunately, this catalyst has a poor selectivity, a wide distribution of products being obtained. Table 4 shows a typical distribution of the hydrocarbons and 4,4-dimethyl-1,3-dioxane obtained when a USY sample was used.

It can be observed that in addition to the condensation of formaldehyde with isobutylene to form isoprene (whatever the route of the reaction from Fig. 1) a large amount of secondary products, such as aromatic hydrocarbons, results. Also, a significant amount of C_1–C_3 aliphatic hydrocarbons is formed (mainly from the cracking of oligomers) but their proportion decreases as the strong acid sites are

TABLE 4

Results of Prins Condensation over USY-80 (Si/Al = 40) at 573 K

Products	2nd pulse	10th pulse
Conversion of isobutylene (%):	76.8	60.7
Distribution of products (wt%):		
C_1–C_3	39.0	24.0
C_4	23.2	39.3
Isoprene	4.0	6.6
C_6–C_8 aliphatics	3.7	2.9
Aromatics	25.2	25.4
DMD[a]	4.7	1.7
Distribution of aromatics (wt%):		
Benzene	5.30	6.8
Toluene	5.4	6.8
Xylenes + ethylbenzene	29.8	37.0
C_{9+}	59.6	49.4

[a] DMD, 4,4-dimethyl-1,3-dioxane.

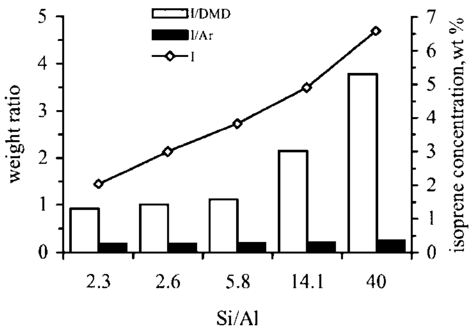

FIG. 7. Isoprene (I) to 4,4-dimethyl-1,3-dioxane (DMD) and aromatics (Ar) weight ratio and Isoprene weight fraction in the products after Prins condensation over H-Y zeolites of various Si/Al ratio, $T = 573$ K; average value of 9–11th pulses.

progressively poisoned by coke (see the second column of Table 4). The high content of hydrocarbons in the products is due to the presence of rather strong acid sites. The significant fraction of bulky C_{9+} aromatics must also be associated with the supercages of faujasites, cages which provide sufficient space for their formation. A part of these products results from the oligomerization and aromatization of olefins. Another part could also result from the disproportionation of xylenes (18).

In their early study, Venuto and Landis (2) have tested a single sample of Y faujasite. Their initial conclusion was that the desired selectivity would only be achieved by a proper choice of pore size. As shown in Fig. 7, another factor, namely the Si/Al ratio has a very important influence on selectivity.

Our previous characterization of the same samples performed by IR, XPS, and NH_3–TPD showed that the concentration of Brønsted acid sites decreases in the order HNaY > USY-5.2 > USY-11.5 > USY-80 (18). In other words, as expected, the Brønsted acid site concentration decreases as the Al content is decreased. It is seen from Fig. 7 that both the isoprene to dimethyldioxane (I/DMD) and the isoprene to aromatics (I/Ar) weight ratios increase as the Si/Al ratio increases. This suggests that a decreased concentration of Brønsted acid sites favors the selectivity to isoprene. The ultrastabilization process, however, changes not only the Si/Al ratio but also the acid strength distribution. Both factors may therefore affect the selectivity. Moreover the low value observed for the I/Ar ratio (well below 1) indicates a severe aromatization of olefins. These results show that a decrease in the strength of the Brønsted acid sites is required in order to improve the selectivity to isoprene in the Prins condensation of isobutylene and formaldehyde.

Prins Condensation over H-ZSM-5 Zeolites

Some improvement of the isoprene selectivity was achieved by using ZSM-5 zeolites instead of Y zeolites as catalysts for Prins condensation. It is well known that the framework aluminum from ZSM-5 is responsible for the formation of strong acid sites which play the role of active sites for various reactions and that the pore structure of ZSM-5 leads to various types of shape selectivity: reactant shape selectivity, product shape selectivity, transition-state shape selectivity (19). Moreover, this zeolite has a longer catalyst life than the Y faujasites due to its resistance to coking.

Thus, Chang *et al.* (3) were the first to show that the formation of DMD can be suppressed due to the molecular size constraint imposed by the pore system of ZSM-5. However, secondary reactions of olefins cannot be avoided.

Our results confirm these findings. In the experiments reported in Table 5, for example, no DMD was detected but the selectivity to isoprene is still low, even lower than in the presence of USY-80. Compared to the data shown in Table 4 for USY-80, the fraction of aromatics in the products is decreased as well as the percent of C_{9+} in the aromatics. The I/Ar weight ratio is still low but when the test was conducted with H-ZSM-5 samples of higher Si/Al ratio (Fig. 8a), this ratio increased dramatically, reaching a value close to 6 at Si/Al = 500. The conversion of isobutylene is, however, decreased due to the decreasing number of acid sites (Fig. 8b). It is well known that as the silicon to aluminum ratio of H-ZSM-5 is increased, the concentration of Brønsted acid sites decreases, but the strength of the acid sites is only mildly affected.

Prins Condensation over H-Boralites

Taking into account the above results, further investigations were focused on boralites, since this kind of molecular sieve is recognized as a weak acid catalyst. Indeed, the Prins condensation has been performed using samples of H-boralites with different boron content (see Table 2) and

TABLE 5

Results of Prins Condensation over HZSM-5 (Si/Al = 17.5) at 573 K

Products	2nd pulse	10th pulse
Conversion of isobutylene (%):	nd	37.2
Distribution of products (wt%):		
C_1–C_3	65.9	17.3
C_4	14.5	60.7
Isoprene	1.6	3.9
C_6–C_8 aliphatics	3.6	1.0
Aromatics	14.4	17.0
Distribution of aromatics (wt%):		
Benzene	3.16	2.2
Toluene	18.2	14.7
Xylenes + ethylbenzene	48.9	56.9
C_{9+}	29.7	26.2

Note. nd, not determined.

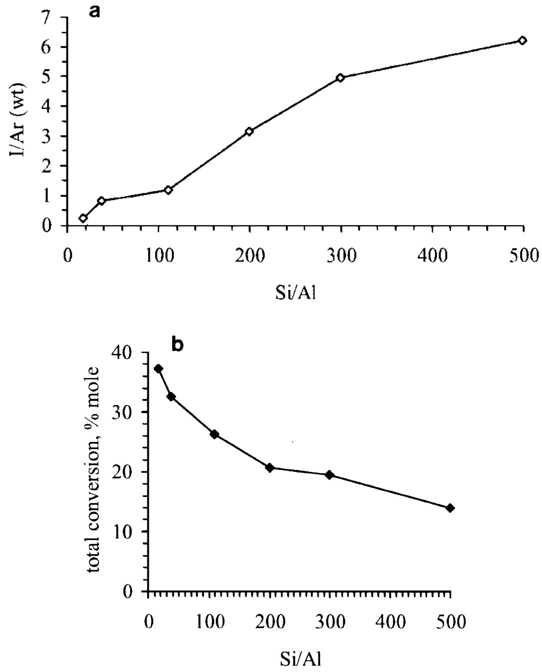

FIG. 8. (a) Isoprene to aromatics (I/Ar) weight ratio and isobutylene conversion vs Si/Al in H-ZSM-5 zeolites; $T = 573$ K, 10th pulse. (b) Overall conversion of isobutylene vs Si/Al ratio at 300C, 10th pulse.

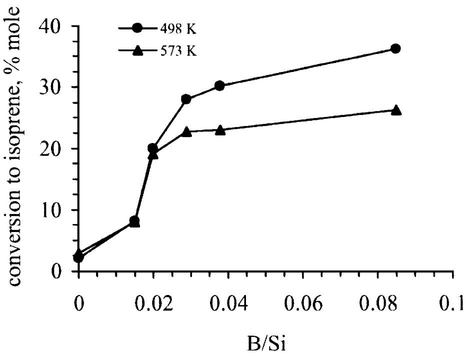

FIG. 10. The influence of boron content of H-boralites on the conversion to isoprene: 30 ml/min flowrate of N_2.

all samples showed a high selectivity to isoprene (∼100%) over a large range of temperature.

Figure 9 shows the conversion to isoprene obtained (average of second and third pulses) with the H-boralite sample, [H]BS-2.9 at various temperatures over the range 448–663 K. A maximum conversion is observed at 473 K. Above this temperature, the conversion decreases smoothly. It must be underlined that these conversions are also isobutylene total conversions as the selectivity is essentially 100% for all these tests. Thus compared to ZSM-5, boralites seem to be of much higher interest for industrial application both because of their high selectivity and their low operation temperature.

A series of experiments have been conducted using boralite samples with various boron contents, the condensation reaction was carried out at two different temperatures, namely 498 and 573 K. These results were compared with those obtained over silicalite (the sample without boron), and they are shown in Fig. 10 (average values of pulse 2–4).

The results in Fig. 10 indicate that the conversion to isoprene increases steeply as the boron content is raised to 4%, which is the isomorphous substitutional limit for boron in boralites (10). Above this limit only a minor increase is observed, indicating that extraframework boron has essentially no activity.

The influence of contact time on the conversion to isoprene was also investigated. The contact time was varied by changing of the carrier gas flow rate, over the range 20–60 ml · min^{-1}. The results are shown in Fig. 11 for [H]BS-2.9 and H-ZSM-5, and they indicate that the conversion to isoprene generally increases as the contact time is decreased. There is, however, a difference in behavior between the two catalysts. Over H-boralite, the conversion shows a uniform and slight increase as the contact time is decreased. For HZSM-5 ($SiO_2/Al_2O_3 = 35$), a maximum is observed at about 40 ml · min^{-1}, after which a slight decrease in conversion occurs.

An increase in reaction rate with flow rate is usually diagnostic for external mass transfer limitations. This may therefore be the case with the H-boralite sample, but the

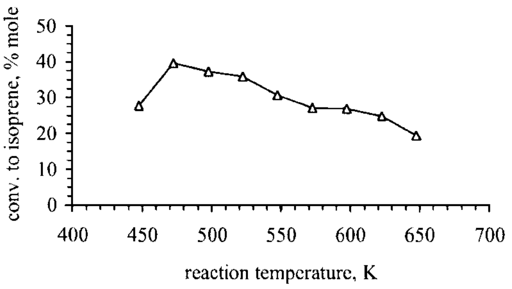

FIG. 9. Conversion to isoprene over H-boralites vs reaction temperature; mole ratio FA/iB=1/1.

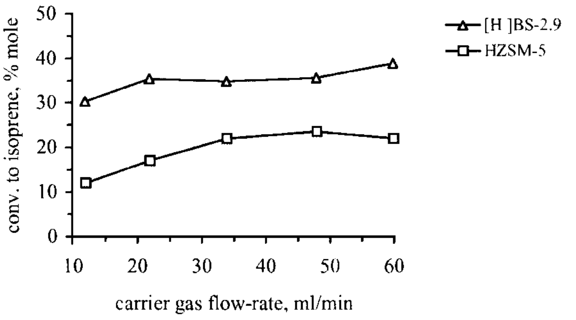

FIG. 11. Conversion of isobutylene to isoprene over H-boralite and H-ZSM-5 (Si/Al = 17.5) vs carrier gas flowrate, reaction temperature 501 K.

situation is less clear with the H-ZSM-5 tests, where selectivity to isoprene is not 100% and the secondary reactions of olefins are also affected by the change is contact time.

The change in conversion with varying molar ratio of reagents in the feed was further studied over [H$^+$]BS-2.9 catalyst, at 498 K. In Fig. 12 the conversion to formaldehyde is reported since isobutylene was in excess.

The conversion of formaldehyde increases significantly (more than twice) as the mole ratio of isobutylene to formaldehyde is increased. Thus both high conversions and 100% selectivity can be simultaneously achieved. This catalytic performance is better than those previously reported for H-ZSM-5 (7), and it may be considered as interesting for industrial application.

Prins Condensation over H-B MCM-41

MCM-41 material is one of the members of the relatively new class of siliceous mesoporous materials M41S (16, 20). This material has attracted much attention due to its hexagonal arrangement of unidimensional pores, varying in size from around 15 Å to more than 100 Å. By comparison with zeolites, this material opens new possibilities for processing large molecules. Moreover, its acid properties can be modified by the substitution of silicon with boron (11, 12).

Therefore, taking into account both its very mild Brønsted acidity and large pore opening, B-MCM-41 has been tested as catalyst for the Prins condensation of formaldehyde with isobutylene. The experiments were performed over the range of temperatures 448–623 K, and the conversion to isoprene results are shown in Fig. 13.

The conversion to isoprene is lower than the ones obtained using boralites. The selectivity, however, is kept at the highest level (100%). It is interesting to note that even though the catalyst has very large pores, 4,4-dimethyl-1,3-dioxane was not observed as a reaction product. This result suggests that the DMD route to isoprene (see Fig. 1) requires stronger Brønsted acid sites than the one present in B-MCM-41. Temperature influences the conversion to isoprene in a manner similar for boralites, since as reported in Fig. 13, a smoothly decreasing conversion is obtained as temperature is raised. It is believed that this minor decrease is due to partial hydrolysis of some Si–O–B bridges under the influence of the water vapor generated by the reaction (11, 12).

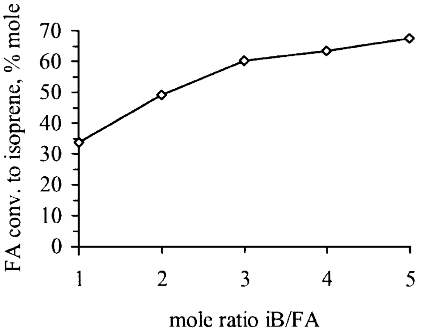

FIG. 12. Influence of mole ratio of reagents in feed on conversion to isoprene over H-boralite ([H]BS-2.9) $T = 500$ K, carrier gas (N_2) flowrate: 30 ml · min^{-1}.

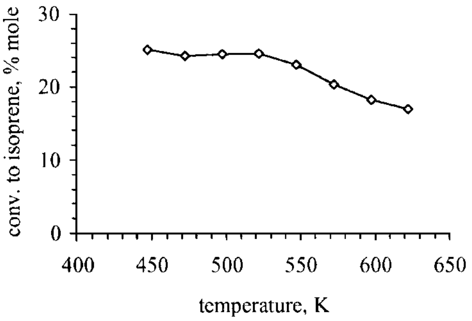

FIG. 13. Conversion to isoprene over B-MCM-41 vs reaction temperature; mole ratio FA/iB = 1/1.

DISCUSSION

In order to appreciate the role of the acid catalytic sites in the isoprene synthesis by Prins condensation, the reactivity of the species involved in this process must first be considered. As shown in Fig. 14, the charge density of the most important reactive species—formaldehyde, isobutene, and isoprene—was calculated (CNDO/2), and based on these data their reactivity has been interpreted.

The most important observation which could be drawn from this Fig. 14 consists of the following order of the polarization of unsaturated linkages:

$$\rangle C{=}O > \rangle C{=}CH_2 > {=}\rangle C{=}CH_2$$

Since oxygen is more electronegative than carbon, formaldehyde shows a dipole moment, and sometimes the carbonyl group is best represented as a hybrid structure, with charges at both atoms. Therefore, due to its bipolar nature, the addition to the carbonyl linkage can be easily initiated by the attack of an electrophile to the oxygen atom, such as the proton from a Brønsted acid site, as depicted in Scheme 1.

As the formed cation (b) can be added to the double bond of isobutylene, the reaction network from Fig. 1 is initiated: of course, other types of reactions are also initiated such as the reactions of electrophilic substitution (e.g., the alkylation of aromatic hydrocarbons, etc.) or the attack of a nucleophile (Nu$^{(-)}$ or Nu:) on the carbon of the carbonyl group.

Regarding the reactivity of isobutylene, due to the π electrons, the olefin might be adsorbed at a protonic acid site even at low temperature, forming a very reactive π complex (see Scheme 2).

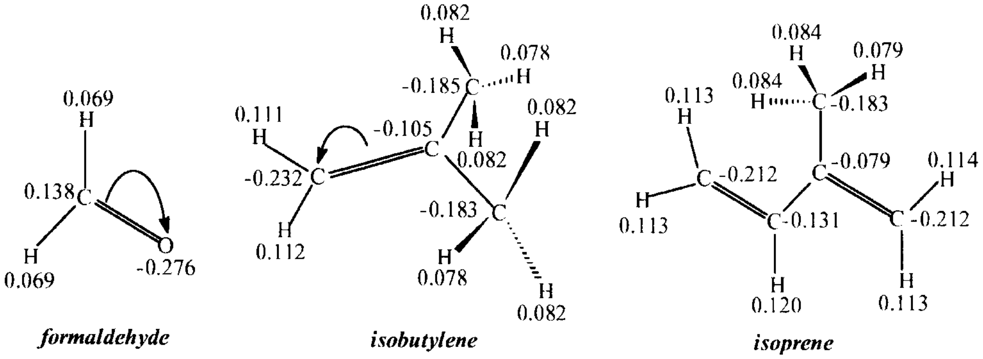

FIG. 14. Charge density of the reagents.

Carbocation (b in Scheme 2) may further react in the following ways: addition to an unsaturated linkage, intermolecular hydride transfer, attack of a nucleophile, etc. Continued structural transformations, such as cyclization, ring contraction, and ring expansion, can also occur. Therefore, a parallel network of reactions involving the unsaturated compounds in various processes such as oligomerization, cracking, aromatization, dealkylation, alkylation, and isomerization could take place. All these pathways are acid-catalyzed reactions which can easily proceed on zeolite catalysts.

The catalytic sites in aluminosilicate zeolites are associated with tetrahedral aluminum atoms in substitutional positions in the framework of silica. The acid strength of the bridging hydroxyls in zeolites, Si–OH–Al, depends both on the geometry of the bridge (bond distances and bridge bond angle) and on the number of Al atoms close to the bridge. The effect of increasing OH dissociation energies for increasing Al content close to the bridging hydroxyl has been discussed by Kazansky (21). A given acidic zeolite usually does not have a single class of acidic sites, but normally shows a distribution of acid strengths. Thus various molecular species can be activated and different reactions may occur. In consequence, the selective synthesis of isoprene, by the condensation of formaldehyde with isobutylene over acid molecular sieves, is a difficult task since both the formation of DMD and aromatic hydrocarbons must be suppressed.

Y zeolite possesses a large distribution of acid strengths, and a system of supercages, connected by a tridimensional array of large-diameter channels, which enables a much easier diffusion of reactants and products, favoring a high activity. The condensation performed on HY faujasite leads to a large distribution of products (2). When the condensation reaction is carried out over USY a wide distribution of products also results, but the proportion of DMD and aromatic hydrocarbons decreases as the Si/Al ratio increases (see Table 4 and Fig. 7). An explanation for this behavior is given below.

The proportion of weak and strong sites changes substantially in the case of USY. Macedo *et al.* (22), as well as other authors (23, 24), studying HY zeolites dealuminated by steaming, found that the strength of intermediate sites decreased with increased dealumination for Si/Al ratios from 8 to higher than 100. Also, Yaluris *et al.* (25) found from differential heats of ammonia adsorption that the acid site strength distribution shifts toward weaker sites when the catalyst is steamed. Steaming results in the preferential loss of Brønsted acid sites. This conclusion agrees with earlier work (24) indicating that the sites of intermediate strength in Y zeolites are predominantly Brønsted acids and their number and strength are reduced with steaming. As Brønsted acid strength decreases, the fractional carbenium ion coverage on USY decreases; strong Brønsted acidity is indeed necessary to stabilized carbenium ions on the surface. Changes in coverage have a direct effect on selectivity. Also, a decrease of unit cell size by steaming, which affects the selectivity, might be considered, even though this effect is not likely to be significant.

Taking into account the above-mentioned data, obtained over Y zeolites, two main factors could be considered in order to achieve a selective synthesis of isoprene: the size of pores, which must be smaller, and the acid properties of the catalyst as the acidity of catalyst must be shifted toward weaker acid strength.

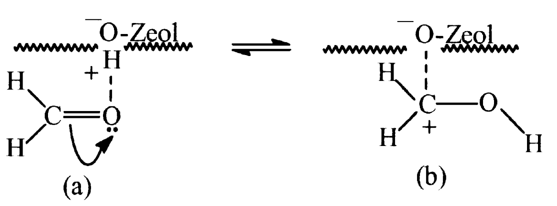

SCHEME 1

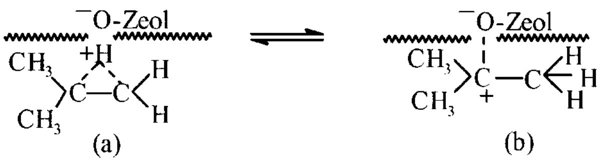

SCHEME 2

The influence of these factors on the selectivity in the Prins condensation must now be examined for MFI catalysts. It is well established that Al-ZSM-5 zeolite has two types of Brønsted acid sites (26), one strong and one weak site in smaller concentration. Therefore, a variety of reactions from both reaction networks can be initiated. Moreover, it is known that due to the strong Brønsted acid sites the reactive olefins can react rapidly even at room temperature to form large oligomers (27, 28). The reactivity of the alkenes increases as the stability of the carbenium ion formed is increased. The oligomers crack to form a large number of products, beginning at ~400 K, and this cracking temperature for the oligomers is an additional measure of the site activity (27). Since the cracking activity depends on the strength of the acid site, it can be considered as a measure for the acid properties of the catalyst. As previously reported (6) the cracking activity disappears as the strong acid sites are blocked by coke. Thus the selectivity increases as the acid strength decreases. Also we demonstrated by progressive poisoning of acid sites by pyridine (6) that a high selectivity to isoprene can be achieved when the catalyst possesses only weak to medium acid strength. This was also confirmed when the silica to alumina ratio was increased (7), but unfortunately the conversion strongly decreased due to the decrease in active sites concentration. The results obtained in the Prins reaction performed over H-ZSM-5 catalysts clearly revealed that the formation of DMD can be suppressed (presumably due to the pore structure) and that most secondary reactions of olefins can be diminished or suppressed by decreasing the acid strength of the catalytic site. Like the faujasites, MFI catalysts having strong acid sites activate both reagents to the corresponding cations (see Schemes 1 and 2), and therefore various reaction routes are opened. In conclusion, it is necessary to modify the acidity of these zeolites in order to achieve selectivity for isoprene in the Prins reaction and one way of doing this is the isomorphous replacement of Al by other trivalent ions.

It has been shown that the isomorphous substitution of silicon by Al, Ga, Fe, and B resulted in a decreasing Si–OH–M acid site strength in this series, as followed by the reactions of paraffin cracking, temperature maxima of ammonia desorption in the temperature-programmed mode, and IR frequency of bridging Si–OH–M groups (29–36) shifting to higher-frequency values. Quantum chemical *ab initio* calculations of simple models of Si–OH–M groups have confirmed (37) that the dissociation energy increased and, thus, the acidity of the proton of the Si–OH–M group decreased in the order Al > Ga > Fe > B.

Our results obtained for Prins condensation carried out over boralites reveal that the isoprene can be selectively synthesized, with reasonable yields. The selectivity of boralites could be explained as follows. It can be assumed that on the weak acid sites of boralites only the carbonyl group is activated leading to the reactive cation (b in Scheme 1), whereas the isobutylene is mainly π-adsorbed on the surface of catalyst (see Scheme 2, species (a)). As is obvious from the high selectivity to isoprene observed, all secondary reactions of olefins are suppressed and the π-adsorbed isobutylene can only react to produce the tertiary carbocation described in Fig. 1. Moreover this cation must desorb rapidly from the weak SiOHB site leaving no time for its reaction with either formaldehyde or water (routes (a) and (c) in Fig. 1). Thus only route (b) is responsible for the formation of isoprene.

The instability of boron during calcination of template containing B-MFI is well known (36, 38, 39) and could be a problem for industrial application of boralites in the Prins condensation. However, Kuehl (40) reported highly stable lattice boron (<5% loss) upon heat treatment of boron-containing molecular sieves is an ammonia atmosphere. This was also confirmed by van Bekkum *et al.* (15) and Trong On *et al.* (10).

Up to this point the selectivity to isoprene may have been considered to be governed by two factors: (i) the size of pores, which acts suppressing the formation of bulky products such as DMD and C_{9+} aromatics, and (ii) the acid strength of the active sites. However, as the results obtained over B-MCM-41 showed, a high selectivity may be achieved, even if the catalyst has large pores, but the active sites are characterized by a weak acid strength. Therefore, we can assume that the acid strength of the catalytic sites is the main factor which governs the selectivity in the Prins condensation.

CONCLUSION

The isoprene synthesis by Prins condensation of isobutene with formaldehyde was studied over a series of catalysts characterized by various pore geometry and acid properties. Results obtained with strongly acidic USY and H-ZSM-5 catalysts showed low selectivity to isoprene and suggested that both pore size and acid strength were two factors affecting this selectivity. Work performed with 10 oxygen ring, weakly acidic boralites showed a spectacular increase in selectivity. The absence of DMD in the products was observed in boralites and in B-MCM-41 as well which indicated that the DMD route to isoprene was not suppressed due to steric constraints or shape selectivity but due to the low acid strength of the catalytic sites. Thus acid strength appears as the most important factor affecting the selectivity of this process.

It is believed that the high selectivity of isoprene formation is reached when the Brønsted acid sites are weak enough so that the protonation of formaldehyde (Scheme 1) is made selectively and no olefin protonation to carbocations (Scheme 2) occurs.

The best isoprene yields have been obtained over boralites (H^+ form), when the selectivity reached approximately 99–100%, and high conversions of up to ∼40% were achieved at low temperatures, around 498 K. It was also found beneficial to carry out the condensation reaction in the presence of an excess of isobutylene.

REFERENCES

1. Noller, C. R., “Chemistry of Organic Compounds,” 3rd ed., W. B. Saunders, Philadelphia/London, 1965.
2. Venuto, P. V., and Landis, P. S., *Adv. Catal.* **18**, 259 (1968).
3. Chang, C. D., Lang, W. H., and Bell, W. K., “Catalysis of Organic Reactions” (W. R. Moser, Ed.), p. 73. Dekker, New York, 1981.
4. Ai, M., *J. Catal.* **106**, 273 (1987).
5. Holderich, W. F., Hesse, M., and Naumann, F., *Angew. Chem. Int. Ed. Engl.* **27**, 226 (1988).
6. Dumitriu, E., Gongescu, D., and Hulea, V., *in* “Heterogeneous Catalysis and Fine Chemicals III” (M. Guisnet, J. Barbier, J. Barrault, C. Bouchoule, D. Duprez, G. Perot, and C. Montassier, Eds.), p. 669. Elsevier, Amsterdam, 1993.
7. Dumitriu, E., Hulea, V., Chelaru, C., Hulea, T., and Kaliaguine, S., *in* “Zeolites and Related Microporous Materials: State of the Art 1994” (J. Weitkamp, H. G. Karge, H. Pfeifer, and W. Holderich, Eds.), p. 1997. Elsevier, Amsterdam, 1994.
8. Venuto, P. B., *Microporous Mater.* **2**, 297 (1994).
9. Trong On, D., Kaliaguine, S., and Bonneviot, L., *J. Catal.* **157**, 235 (1995).
10. Trong On, D., Kapoor, M. P., Bonneviot, L., Kaliaguine, S., and Gabelica, Z., *J. Chem. Soc. Faraday Trans.* **92**, 1031 (1996).
11. Trong On, D., Joshi, P. N., Lemay, G., and Kaliaguine, S., *Stud. Surf. Sci. Catal.* **97**, 543 (1995).
12. Trong On, D., Joshi, P. N., and Kaliaguine, S., *J. Phys. Chem.* **100**, 6743 (1996).
13. Meyers, B. L., Ely, S. R., Kutz, N. A., Kaduk, J. A., and Van Den Bossche, E., *J. Catal.* **91**, 352 (1985).
14. Kessler, H., Chezeau, J. M., Guth, J. L., Strub, H., and Coudurier, G., *Zeolites* **7**, 360 (1992).
15. de Ruiter, R., Kentgens, A. P. M., Grootendorst, J., Jansen, J. C., and van Bekkum, H., *Zeolites* **13**, 128 (1993).
16. Kresge, C. T., Leonowicz, M. E., Roth, W. J., Vartuli, J. C., and Beck, J. S., *Nature* **359**, 710 (1992).
17. Ghosh, A. K., and Curthoys, G., *J. Chem. Soc. Faraday Trans. 1* **79**, 805 (1983).
18. Dumitriu, E., Hulea, V., Kaliaguine, S., and Huang, M. M., *Appl. Catal. A* **135**, 57 (1996).
19. Chen, N. Y., Garwood, W. E., and Dwyer, F. G., “Shape Selective Catalysis in Industrial Applications.” Dekker, New York, 1996.
20. Beck, J. S., Vartuli, J. C., Roth, W. J., Leonowicz, M. E., Kresge, C. T., Schmitt, K. D., Chu, T. U., Olsen, D. H., Sheppard, E. W., McCullen, S. B., Higgins, J. B., and Schlenker, J. L., *J. Am. Chem. Soc.* **114**, 10834 (1992).
21. Kazansky, V. B., “Structure and Reactivity of Modified Zeolites,” p. 61. Elsevier, Amsterdam, 1984.
22. Macedo, A., Auroux, A., Raatz, F., Jacquinot, E., and Boulet, R., *in* “Perspectives in Molecular Sieve Science” (W. H. Flank and T. E. Whyte, Jr., Eds.), p. 98, ACS Symposium Series, Vol. 368. American Chemical Society, Washington, DC, 1988.
23. Auroux, A., and Ben Taarit, Y., *Therm. Acta* **122**, 63 (1987).
24. Chen, D., Sharma, S., Cardona-Martinez, N., Dumesic, J. A., Bell, V. A., Hodge, G. D., and Madon, R. J., *J. Catal.* **136**, 392 (1992).
25. Yaluris, G., Rekoske, J. E., Aparicio, L. M., Madon, R. J., and Dumesic, J. A., *J. Catal.* **153**, 65 (1995).
26. Borade, R. B., Adnot, A., and Kaliaguine, S., *J. Phys. Chem.* **94**, 5989 (1990).
27. Kofke, T. J. G., and Gorte, R. J., *J. Catal.* **115**, 233 (1989).
28. Dimitrov, Chr., and Bezouhanova, C. P., *in* “Catalysis by Zeolites” (D. Kallo and Kh. M. Minachev, Eds.), p. 95. Akadémiai Kiadó, Budapest, 1988.
29. Chu, C. T.-W., and Chang, C. D., *J. Phys. Chem.* **89**, 1569 (1985).
30. Datka, J., and Kawalek, M., *J. Chem. Soc. Faraday Trans.* **89**, 1829 (1993).
31. Scholle, K. F. M. J. G., Kentgens, A. P. M., Veeman, W. S., Frenken, P. F., and Ven der Velden, G. P. M., *J. Phys. Chem.* **88**, 5 (1984).
32. Kofke, T. J. G., Gorte, R. J., and Kokotailo, G. T., *J. Catal.* **116**, 252 (1989)
33. Chu, C. T.-W., Kuehl, G. H., Lago, R. M., and Chang, C. D., *J. Catal.* **93**, 451 (1985).
34. Sayed, M. B., Auroux, A., and Vedrine, J. C., *J. Catal.* **116**, 1 (1989).
35. Kutz, N. A., *in* “Perspectives in Molecular Sieve Science” (W. H. Flank and T. E. Whyte, Eds.), p. 532, ACS Symposium Series, Vol. 368. American Chemical Society, Washington, DC, 1988.
36. Beyer, H. K., and Borbely, G., *in* “New Developments in Zeolite Science and Technology” (Y. Murakami, A. Ijima, and J. W. Ward, Eds.) p 867. Proceedings of the 7th International Zeolite Conference Kodansha, Tokyo, 1986.
37. Zahradnik, R., Hobza, P., Wichterlova, B., and Cejka, J., *Coll. Czech. Chem. Commun.* **58**, 2474 (1993).
38. Brunner, E., Freude, D., Hunger, M., Pfeifer, H., Reschetilowski, W., and Unger, B., *Chem. Phys. Lett.* **148**, 226 (1988).
39. Cichocki, A., Lasocha, W., Michalik, M., Sawlowicz, Z., and Bus, M., *Zeolites* **10**, 583 (1990).
40. Kuehl, G. H., U.S. Patent 4,661,467 (1987).